

surface as determined by  $^1\text{H}$  NMR and  $\rho_a$  and  $\rho_c$  are the amorphous and crystalline densities, respectively. An  $L_c$  value of 4.98 nm is found from eq 5. The crystal thickness can be estimated from our value of the stem length by multiplying  $L_s$  and the sine of the angle of inclination for the crystalline stem. If we assume the fold surface is in the 001 plane, the chain tilt will equal the  $\beta$  angle in the unit cell ( $102^\circ$ ) for the  $\alpha$  form.<sup>21</sup> This gives an  $L_c$  value of 4.81 nm. However, it should be noted that crystals grown in the manner employed in this work can be curved or cup-shaped, in which case the crystal-growth plane may not be 001.

## Conclusions

The method of nondestructive chemical transformation of surface folds followed by high-resolution carbon-13 NMR analysis is demonstrated to be a direct quantitative measure of the surface folds, the crystalline stems, and the fraction crystallinity in solution-grown polymer crystals. This approach should be applicable to other polymer systems in which a suitable chemical treatment can be established.

The values of fold length,  $U$ , and stem length,  $L_s$ , determined quantitatively from our carbon-13 results for one preparation of TPI crystals, are in excellent agreement with those reported previously based on determinations of surface fraction, crystal and amorphous densities, and the monomer repeat distance.<sup>8</sup> Together these studies present a detailed picture of the morphology of TPI solution-grown crystals.

Results of additional studies on TPI crystalline preparations employing this analytical approach will be presented in a subsequent report. This will include the analysis of the dissolution properties of various suspension liquids employed in the crystal epoxidation of TPI and the effects of crystallization temperature on chain folding. In addition, results of carbon-13 NMR solid-state studies on the  $\alpha$  and  $\beta$  forms of TPI will be reported in the near future.

**Acknowledgment.** The City College portion of this work was supported by the National Science Foundation, Polymers Program.

Registry No. Squalene, 111-02-4.

## References and Notes

- (1) Keller, A. *Faraday Discuss. Chem. Soc.* **1980**, *68*, 145.
- (2) Wunderlich, B. "Macromolecular Physics"; Academic Press: New York, 1973; Vol. 1, 208, 454.
- (3) Williams, T.; Blundell, D. J.; Keller, A.; Ward, I. M. *J. Polym. Sci., Part A-2* **1968**, *6*, 1613.
- (4) Williams, T.; Keller, A.; Ward, I. M. *J. Polym. Sci., Part A-2* **1968**, *6*, 1621.
- (5) Keller, A.; Martuscelli, E.; Priest, D. J.; Udagawa, Y. *J. Polym. Sci., Part A-2* **1971**, *9*, 1807.
- (6) Schilling, F. C.; Bovey, F. A.; Tseng, S.; Woodward, A. E. *Macromolecules* **1983**, *16*, 808; *Polym. Prepr. (Am. Chem. Soc., Div. Polym. Chem.)* **1983**, *24* (1), 235.
- (7) Schilling, F. C.; Bovey, F. A.; Tonelli, A. E.; Tseng, S.; Woodward, A. E. *Macromolecules* **1984**, *17*, 728.
- (8) Anandakumaran, K.; Herman, W.; Woodward, A. E. *Macromolecules* **1983**, *16*, 563.
- (9) Kuo, C.; Woodward, A. E. *Macromolecules* **1984**, *17*, 1034.
- (10) Anandakumaran, K.; Kuo, C. C.; Mukherji, S.; Woodward, A. E. *J. Polym. Sci., Polym. Phys. Ed.* **1982**, *20*, 1669.
- (11) Levitt, M. H.; Freeman, R. J. *Magn. Reson.* **1979**, *33*, 473.
- (12) Corey, E. J.; Russey, W. E.; Ortiz de Montellano, P. R. *J. Am. Chem. Soc.* **1966**, *88*, 4750. van Tamelen, E. E.; Willet, J. D.; Clayton, R. B.; Lord, K. E. *Ibid.* **1966**, *88*, 4752.
- (13) Grant, D. M.; Paul, E. G. *J. Am. Chem. Soc.* **1964**, *86*, 2984.
- (14) Lindemann, L. P.; Adams, J. Q. *Anal. Chem.* **1971**, *43*, 1245.
- (15) Pegg, D. T.; Doddrell, D. M.; Bendall, M. R. *J. Chem. Phys.* **1982**, *77*, 2745.
- (16) Sorenson, O. W.; Ernst, R. R. *J. Magn. Reson.* **1983**, *51*, 477.
- (17) Gemmer, R. V.; Golub, M. A. *J. Polym. Sci., Polym. Chem. Ed.* **1978**, *16*, 2985.
- (18) In considering a sequence of three oxirane rings in TPI the four diastereoisomers are as follows:  $R_2R_3-R_2R_3-R_2R_3$ ;  $R_2R_3-R_2R_3-S_2S_3$ ;  $S_2S_3-R_2R_3-R_2R_3$ ;  $S_2S_3-R_2R_3-S_2S_3$ . The  $R$  and  $S$  designations represent the chirality of either carbon 2 or carbon 3. Of course, a set of four enantiomers exists in which we interchange all  $R$  and  $S$  designations in the four sequences above. However, NMR cannot normally distinguish such enantiomers in the absence of a chiral shift reagent or chiral solvent.
- (19) Hayashi, O.; Takahashi, T.; Kurihara, H.; Ueno, H. *Polym. J. (Tokyo)* **1981**, *13*, 215.
- (20) Takahashi, Y.; Sato, T.; Tadokoro, H.; Tanaka, Y. *J. Polym. Sci., Polym. Phys. Ed.* **1973**, *11*, 233.
- (21) Fisher, D. *Proc. Phys. Soc., London* **1953**, *66*, 7.
- (22) The peaks labeled "x" result from an apparent side reaction in TPI epoxidized to 90% at 20  $^\circ\text{C}$ . It is probable that the MCBA is reacting with oxirane to form an ester linkage and a secondary alcohol.

## Viscosity of Concentrated Solutions of Rodlike Polymers

Harumitu Enomoto, Yoshiyuki Einaga,\* and Akio Teramoto

Department of Macromolecular Science, Osaka University, Toyonaka, Osaka, 560 Japan.

Received May 15, 1985

**ABSTRACT:** Viscosities of aqueous solutions of a triple-helical polysaccharide schizophyllan were measured with four samples of different molecular weights. The data obtained were combined with those reported previously and analyzed theoretically. The seven samples studied consisted of four lower molecular weight samples of rigid-rod shape and three higher molecular weight samples exhibiting flexibility. Zero-shear viscosities  $\eta_0$  increased with  $C^6-C^8$  in a relatively low range of concentration. There was a maximum in the  $\eta_0$  vs.  $C$  curve for each of the lower molecular weight samples.  $\eta_0$  at a fixed concentration increased with  $M^7-M^8$  for the rigid-rod samples and approximately with  $M^6$  for the semiflexible samples. For the former samples, the  $C$  and  $M$  dependence of zero-shear viscosity could be described by Doi's viscosity equation for rodlike polymer solutions when  $\eta_0$  was replaced by  $\eta_a$ , obtained by subtracting the dilute solution contribution  $\eta_d$  from  $\eta_0$ . Here  $\eta_d = \eta_a[1 + C[\eta] + k'(C[\eta])^2]$ , where  $\eta_a$  is the solvent viscosity,  $[\eta]$  the zero-shear intrinsic viscosity, and  $k'$  the Huggins constant. A value of 8.8 was obtained for  $\alpha$ , a numerical parameter in the Doi theory. Doi's viscosity equation predicted the absolute value of  $\eta_a$  accurate to 0.03 relative to unity.  $\eta_a$  was much lower for any of the semiflexible samples than for the corresponding rigid rod at a given  $CM$ , and the difference varied with the degree of flexibility and polymer concentration. A comparison of the schizophyllan data with those of other rigid polymers showed  $\alpha$  not to be universal but characteristic of the polymer-solvent system.

Rodlike polymers disperse randomly in dilute solution, forming an isotropic solution. Above some critical con-

centration  $C_A$ , the solution begins to separate out a liquid crystal phase. The liquid crystal phase increases in volume

with increasing concentration, eventually covering the entire solution above another critical concentration  $C_B$ .<sup>1,2</sup> Owing to the geometrical characteristic of thin, long rodlike shape and the liquid crystal formation, the viscosity behavior of rodlike polymer solutions is greatly different from that of flexible polymer solutions. As for zero-shear viscosity  $\eta_0$  (1)  $\eta_0$  increases with  $C^5$ – $C^8$  with increasing polymer concentration  $C$  at relatively low concentrations,<sup>3–8</sup> (2)  $\eta_0$  increases with  $M$  raised to a power as high as 7–8,<sup>3–6</sup> and (3)  $\eta_0$  as a function of  $C$  reaches a maximum near the boundary concentration between the isotropic and biphasic regions and decreases sharply at higher concentrations.<sup>3,4,7–10</sup>

Taking account of the entanglement effect that long and rodlike molecules cannot pass through each other, Doi<sup>11</sup> derived an expression for  $\eta_0$ . Later he extended his theory to nematic solutions.<sup>12</sup> The Doi theory<sup>11,12</sup> describes well the qualitative features of the viscosity behavior of rodlike polymer solutions noted above. However, there are important problems left unsolved experimentally and theoretically:

(1) Rodlike polymers generally show poor solubility, and slight differences in solvent condition and sample treatment often lead to association.<sup>5,13</sup> Therefore, accurate molecular characterization in dilute solution is a difficult task, and solubility at high concentration must be checked with great care.

(2) As was mentioned above,  $\eta_0$  depends remarkably on  $M$ . Therefore, it is desirable to use samples of narrow molecular weight distribution. However, the samples used in the previous studies either are polydisperse ( $M_w/M_n > 2$ )<sup>4</sup> or have no information about molecular weight distribution.

(3) Chain flexibility should have significant effects on the viscous behavior of polymer solutions because rodlike polymers and flexible polymers differ greatly in this behavior. It is well-known that even a rigid polymer, which is perfectly straight at low molecular weight, appears flexible at high molecular weight. Thus it may be possible to extract the effect of chain flexibility on viscous behavior by examining a homologous series of polymer samples differing widely in molecular weight; in this case all the other conditions can be fixed. This type of approach has not been attempted as yet except in our previous study.<sup>14</sup>

(4) Since the viscosity equation of Doi<sup>11</sup> has been derived omitting most numerical coefficients, it describes the  $C$  and  $M$  dependence of  $\eta_0$  but does not predict the absolute value of  $\eta_0$ . No attempt has been made to estimate the numerical coefficient  $\alpha$  in the Doi theory.

The polysaccharide schizophyllan dissolves well in water, forming a three-stranded helix to take up a rodlike shape. According to Yanaki et al.,<sup>15</sup> schizophyllan with a molecular weight larger than 500 000 exhibits flexibility, although it is remarkably rigid at low molecular weights. One may get available samples with a narrow molecular weight distribution ( $M_w/M_n < 1.2$ ) over a wide range of molecular weight.<sup>15–17</sup> It has been shown that aqueous solutions of schizophyllan form a cholesteric mesophase at high concentration.<sup>17–19</sup> For these reasons, schizophyllan is a polymer suitable to investigate the viscosity behavior of concentrated solutions and the effect of chain flexibility on it.

In our previous paper,<sup>14</sup>  $\eta_0$  of three schizophyllan samples with different molecular weights were measured and the features 1–3 were examined. Four additional samples were studied in the present work. The resulting data along with the previous ones are presented and analyzed on the basis of the Doi theory.

First, we test the validity of the Doi theory using the data for the low molecular weight samples. Comparing these data with those of high molecular weight samples, we make clear the effect of chain flexibility on zero-shear viscosities. As mentioned in problem 3, this is one of the most direct methods to test the effect of chain flexibility. Finally, we investigate whether the Doi theory can consistently explain the viscosity behavior of various rodlike polymers.

## Experimental Section

Sonicated schizophyllan samples supplied by Taito Co. were fractionated by fractional precipitation and gel filtration. For the gel filtration, use was made of two columns 5 cm in diameter and 25 cm in length with Sepharose CL-6B (Pharmacia Fine Chemicals). Appropriate middle fractions having similar intrinsic viscosities were combined to obtain samples R-4, H-23, and S-35; sample R-4 was obtained by fractional precipitation followed by gel filtration and other samples only by fractional precipitation. These samples were freeze-dried from 1–0.1% aqueous solutions filtered through 1–3- $\mu$ m Millipore filters or filter paper (Toyo Kagaku A-5). The native schizophyllan sample stocked in our laboratory was dissolved in water, filtered through filter paper (Toyo Kagaku A-5), reprecipitated into acetone, and dried under reduced pressure to obtain sample N-1.

Solutions were made by mixing the required amounts of a given sample and water in a stoppered flask for 5–7 days at room temperature. The weight fraction  $w$  of the polymer was determined gravimetrically. The mass concentration  $C$  (g cm<sup>-3</sup>) was calculated from  $w$  with the solution density data reported elsewhere.<sup>19</sup> Unless otherwise mentioned, solutions of samples S-35 and N-1 were filtered through filter paper before viscosity measurement and their concentrations were determined by refractometry.

Intrinsic viscosities were measured at 25 °C in water on conventional Ubbelohde type capillary viscometers for samples SPG-4, R-4, and H-23; Ubbelohde low-shear four-bulb capillary viscometers<sup>20</sup> were used for other samples. The apparent shear rate was about 800 s<sup>-1</sup> in the conventional Ubbelohde viscometer and in the range 10–110 s<sup>-1</sup> in the four-bulb viscometer. The data obtained were used to determine the zero-shear intrinsic viscosities  $[\eta]$  of the samples.

Viscosity measurements were made at 30 °C on a Zimm-Crothers type rotational viscometer.<sup>14,21</sup> After each measurement, the polymer solution was diluted with water in the viscometer for the subsequent measurement. At least several original solutions were used for each sample to cover the necessary concentration range.

## Results

**Solubility and Molecular Characterization of Schizophyllan Samples.** Schizophyllan dissolves in water at high concentration (at least higher than 38%) in the form of a triple helix.<sup>19</sup> However, it is indicated<sup>22</sup> that slight aggregation may occur even in a dilute solution; complete dissolution was attained in 0.01 N NaOH. Therefore it was essential to examine if high molecular weight samples would completely dissolve in such concentrated solutions as those used for viscosity measurements. No aggregation problem was encountered with low molecular weight samples SPG-4, R-4, and H-23. When solutions of high molecular weight samples S-25 and N-1 were filtered by filter paper (Toyo Kagaku A-5), their concentrations were found to increase by less than a few percent and their viscosities to decrease by 30% at maximum; no concentration increase was found with dilute solutions used for  $[\eta]$  measurements. At given concentrations, the viscosities of filtered solutions of sample S-35 were substantially in agreement with those of 0.01 N NaOH solutions. Thus we concluded that solutions of samples S-35 and N-1 would be freed from aggregation by filtration. There was no aggregation with samples E-51 and F-52, which might seriously affect viscosity.<sup>14</sup>

Table I  
Molecular Characterization of the Schizophyllan Samples Used

| sample | $[\eta]_0$ ( $[\eta]_R$ ),<br>$\text{cm}^3 \text{g}^{-1}$ | $M_v \times 10^{-3}$ | $L/2q^a$ | $C_A$ ,<br>$\text{g cm}^{-3}$ | $C_B$ ,<br>$\text{g cm}^{-3}$ | $C^{**}$ ,<br>$\text{g cm}^{-3}$ |
|--------|---|----------------------|----------|-------------------------------|-------------------------------|----------------------------------|
| SPG-4  | 64  | 128                  | 0.15     | 0.198                         | 0.243                         | 0.209                            |
| R-4    | 161   | 220                  | 0.26     | 0.141                         | 0.186                         | 0.135                            |
| H-23   | 335   | 340                  | 0.40     | 0.112                         | 0.160                         | 0.112                            |
| E-51   | 541   | 460                  | 0.54     | 0.098                         | 0.146                         |                                  |
| F-52   | 1440 (1940) <sup>b</sup>                                  | 960                  | 1.12     | 0.080                         | 0.126                         |                                  |
| S-35   | 2935 (5300) <sup>b</sup>                                  | 1730                 | 2.02     | 0.072                         | 0.118                         |                                  |
| N-1    | 8800 (26000) <sup>b</sup>                                 | 4300                 | 5.02     | 0.066                         | 0.112                         |                                  |

<sup>a</sup> Calculated from  $L = M/M_L$  with  $M_L = 2140 \text{ nm}^{-1}$  and  $q = 200 \text{ nm}^{-1}$ .<sup>15</sup> <sup>b</sup> Values in the parentheses were read from Figure 6 of ref 15.  $C_A$  and  $C_B$  were estimated from the data of Itou et al.<sup>17</sup>  $C^{**}$  is the mass concentration at which  $\eta_0$  becomes maximum (see Figure 4).

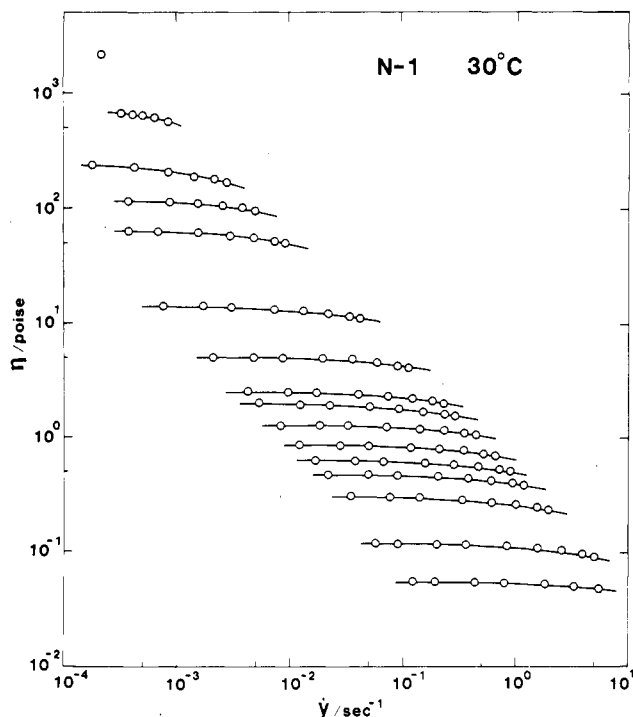


Figure 1. Shear rate dependence of viscosity  $\eta$  for sample N-1 in water at 30 °C. The polymer concentration  $C$  is 0.00411, 0.00313, 0.00284, 0.00246, 0.00216, 0.00159, 0.00125, 0.00104, 0.00102, 0.000894, 0.000796, 0.000716, 0.000652, 0.000551, 0.000378, and 0.000257  $\text{g cm}^{-3}$  from top to bottom.

Viscosity-average molecular weights  $M_v$  were determined from the  $[\eta]$ - $M_w$  relation for aqueous solutions at 25 °C established by Yanaki et al.,<sup>15</sup> where  $M_w$  is the weight-average molecular weight. Table I summarizes the molecular characteristics of the schizophyllan samples investigated. It is seen that  $M_v$  covers a wide range from  $128 \times 10^3$  to  $4300 \times 10^3$ . These samples were obtained by methods similar to those used before, which yielded a polydispersity index  $M_z/M_w$  of about 1.2.<sup>17</sup>  $[\eta]_R$  is the intrinsic viscosity of the corresponding rigid-rod sample calculated on the basis of the analysis by Yanaki et al.,<sup>15</sup> and  $L/2q$  is Kuhn's statistical segment number. For samples SPG-4, R-4, H-23, and E-51,  $[\eta] \approx [\eta]_R$  and  $L/2q < 1$ ; this means that these samples are rigid rodlike. On the other hand,  $[\eta] < [\eta]_R$  and  $L/2q > 1$  for the other samples; that is, they are flexible to some extent.

**Steady-State Viscosity of Aqueous Schizophyllan.** Figure 1 shows the shear rate  $\dot{\gamma}$  dependence of the apparent viscosity  $\eta$  in the isotropic region for sample N-1, where  $\dot{\gamma}$  covers a relatively narrow range from  $10^{-4}$  to  $10^{-1} \text{ s}^{-1}$ . For this sample  $\eta$  at each concentration decreases with increasing  $\dot{\gamma}$ , but the decrease is at most 20%. For the most concentrated solution with  $C = 4.11 \times 10^{-3} \text{ g cm}^{-3}$ , the applied torque was too small to determine the shear rate dependence of  $\eta$ . In no case was hysteresis found in

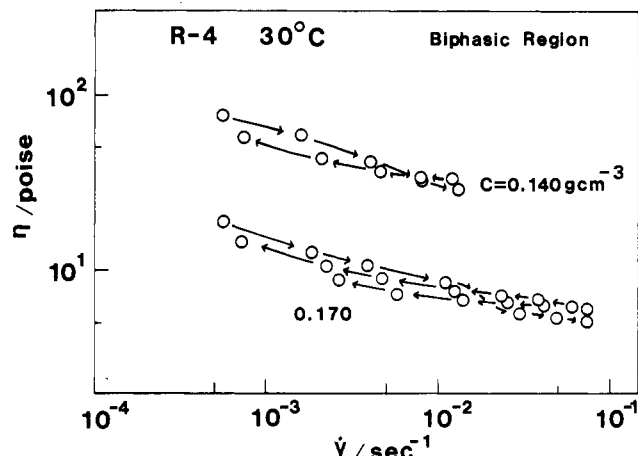


Figure 2. Shear rate dependence of viscosity  $\eta$  for aqueous solutions of sample R-4 at 30 °C in the biphasic region. Arrows indicate the order of measurements.

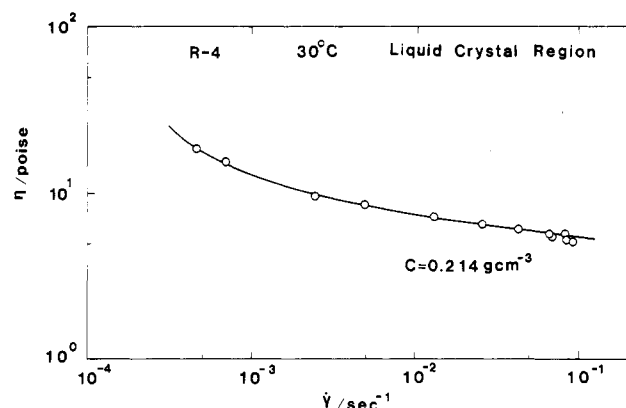


Figure 3. Shear rate dependence of viscosity  $\eta$  for a liquid crystal solution of sample R-4 at 30 °C.

shear flow. For samples R-4, H-23, and S-35,  $\eta$  was almost constant within this range of shear rate. Therefore average  $\eta$  values at low shear rates or those at the lowest shear rate were taken as  $\eta_0$ . The  $\eta_0$  values thus obtained are summarized in Table II.

For samples R-4 and H-23, a series of measurements were made also at concentrations above  $C_A$  with changing torque. Figure 2 shows the result for sample R-4 in the biphasic region. A steady-state value was obtained for  $\eta$  after applying a constant torque for about 20–60 min. The arrows in the figure indicate the order of measurements. The biphasic solutions show hysteresis, yielding no reproducible  $\eta$ . However, at high shear rates each solution exhibits almost constant  $\eta$  each time, which is included as  $\eta_0$  in Table II.<sup>23</sup>

Figure 3 shows similar data for a liquid crystal solution of R-4. This solution shows non-Newtonian behavior but no hysteresis. The  $\eta$  value at the highest shear rate is

**Table II**  
Zero-Shear Viscosities of Aqueous Solutions of  
Schizophyllan at 30 °C

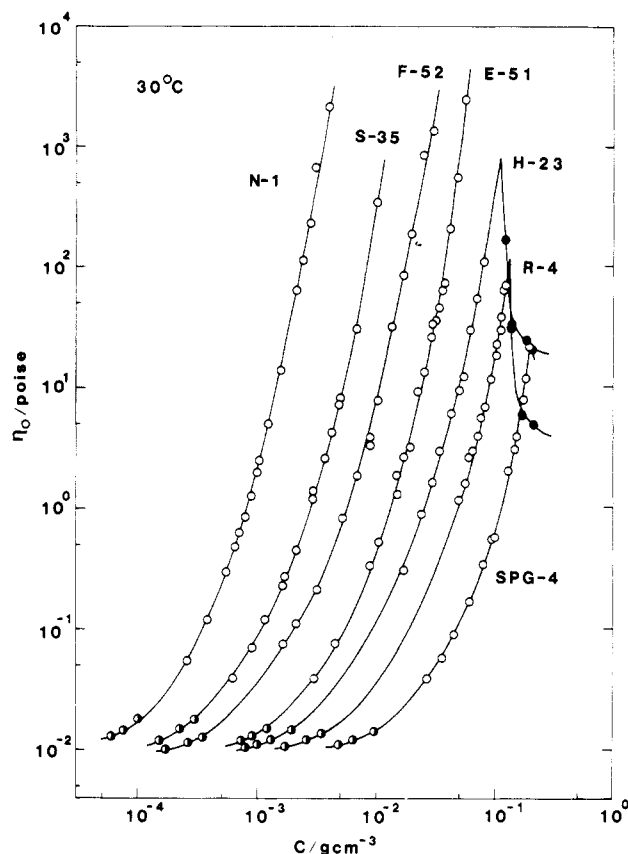
| $C$ , g                | $\eta_0$ , P      | $C$ , g cm <sup>-3</sup> | $\eta_0$ , P |
|------------------------|-------------------|--------------------------|--------------|
| Sample R-4             |                   |                          |              |
| 0.214 <sup>a</sup>     | 5.0               | 0.0832                   | 7.0          |
| 0.170 <sup>a</sup>     | 6.0               | 0.0762                   | 5.66         |
| 0.140 <sup>b</sup>     | 31                | 0.0718                   | 4.04         |
| 0.124                  | 70                | 0.0643                   | 3.0          |
| 0.120                  | 64                | 0.0601                   | 2.64         |
| 0.114                  | 38.6              | 0.0563                   | 1.62         |
| 0.113                  | 29.2              | 0.0496                   | 1.18         |
| 0.105                  | 23                | $3.43 \times 10^{-3}$    | 0.0135       |
| 0.103                  | 18.5              | $2.57 \times 10^{-3}$    | 0.0119       |
| 0.0931                 | 11.8              | $1.72 \times 10^{-3}$    | 0.0104       |
| Sample H-23            |                   |                          |              |
| 0.184 <sup>a</sup>     | 25                | 0.0341                   | 3.02         |
| 0.140 <sup>a</sup>     | 34                | 0.0297                   | 1.66         |
| 0.125 <sup>a</sup>     | 170               | 0.0238                   | 0.91         |
| 0.0822                 | 112               | 0.0169                   | 0.31         |
| 0.0710                 | 55.2              | $1.96 \times 10^{-3}$    | 0.0147       |
| 0.0625                 | 30.1              | $1.31 \times 10^{-3}$    | 0.0121       |
| 0.0548                 | 12.4              | $9.81 \times 10^{-4}$    | 0.0109       |
| 0.0505                 | 9.65              | $7.85 \times 10^{-4}$    | 0.0103       |
| 0.0436                 | 6.08              |                          |              |
| Sample S-35            |                   |                          |              |
| 0.0106 <sup>c</sup>    | 344.7             | $1.69 \times 10^{-3}$    | 0.272        |
| $6.87 \times 10^{-3}$  | 30.9              | $1.65 \times 10^{-3}$    | 0.23         |
| $5.01 \times 10^{-3}$  | 8.36              | $1.17 \times 10^{-3}$    | 0.12         |
| $5.14 \times 10^{-3c}$ | 7.31              | $9.06 \times 10^{-4}$    | 0.07         |
| $4.40 \times 10^{-3}$  | 4.29              | $6.20 \times 10^{-4}$    | 0.039        |
| $3.84 \times 10^{-3}$  | 2.62              | $2.95 \times 10^{-4}$    | 0.0181       |
| $2.97 \times 10^{-3}$  | 1.40              | $2.21 \times 10^{-4}$    | 0.0149       |
| $2.94 \times 10^{-3}$  | 1.20              | $1.48 \times 10^{-4}$    | 0.0121       |
| $2.13 \times 10^{-3}$  | 0.45              |                          |              |
| Sample N-1             |                   |                          |              |
| $4.11 \times 10^{-3}$  | 2164 <sup>d</sup> | $7.96 \times 10^{-4}$    | 0.853        |
| $3.13 \times 10^{-3}$  | 670               | $7.16 \times 10^{-4}$    | 0.63         |
| $2.84 \times 10^{-3c}$ | 230               | $6.52 \times 10^{-4}$    | 0.48         |
| $2.46 \times 10^{-3}$  | 113               | $5.51 \times 10^{-4}$    | 0.30         |
| $2.16 \times 10^{-3}$  | 64                | $3.78 \times 10^{-4}$    | 0.12         |
| $1.59 \times 10^{-3}$  | 14                | $2.57 \times 10^{-4}$    | 0.0547       |
| $1.25 \times 10^{-3}$  | 5                 | $9.85 \times 10^{-5}$    | 0.0180       |
| $1.04 \times 10^{-3}$  | 2.5               | $7.38 \times 10^{-5}$    | 0.0147       |
| $1.02 \times 10^{-3c}$ | 2.0               | $5.91 \times 10^{-5}$    | 0.0130       |
| $8.94 \times 10^{-4}$  | 1.28              |                          |              |

<sup>a</sup> Biphase mixtures. <sup>b</sup> Liquid crystal solution. <sup>c</sup> Solutions filtered through Toyo Kagaku 5A filter paper. <sup>d</sup> Values to be taken with reservations.

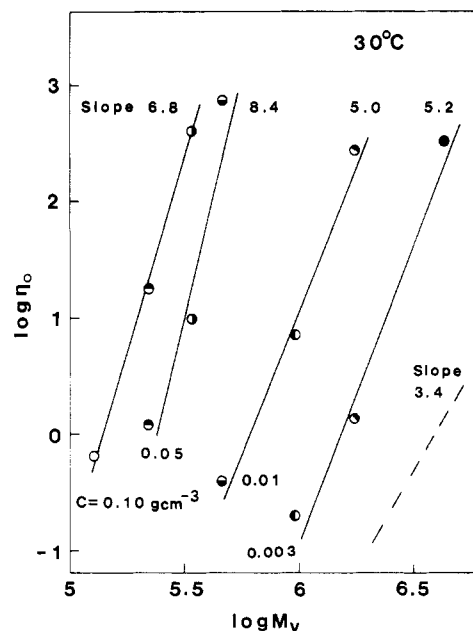
tabulated as  $\eta_0$  in Table II.<sup>23</sup>

Figure 4 shows double-logarithmic plots of  $\eta_0$  vs.  $C$  for all the samples investigated; the data for samples SPG-4, E-51, and F-52 have been reproduced from our previous paper.<sup>14</sup> All the plots are almost parallel but displaced toward lower concentration along the abscissa as the molecular weight is increased. For either sample,  $\eta_0$  increases with increasing concentration gradually at lower concentration and sharply at higher concentration. The viscosity curves of samples SPG-4, R-4, and H-23 have maxima. Table I shows that the concentration  $C^{**}$  for the maximum  $\eta_0$  agrees with  $C_A$  within experimental error. This remarkable concentration dependence and the appearance of the maximum confirm the characteristic features 1 and 2 of rodlike polymer solutions so far studied. Matheson<sup>24</sup> suggested from a theoretical consideration that a  $\eta_0$  vs.  $C$  curve would continue to rise above  $C_A$  but with a smaller slope and drop abruptly above some concentration in the biphasic region, and thus  $C_A < C^{**}$ . However, Figure 4 indicates no such transient region to exist in aqueous schizophyllan.

Figure 5 shows double-logarithmic plots of  $\eta_0$  vs.  $M_v$  at fixed concentrations, where the  $\eta_0$  values have been read



**Figure 4.** Concentration dependence of zero-shear viscosity  $\eta_0$  for aqueous solutions of seven schizophyllan samples at 30 °C: open circles, isotropic solutions; filled circles, biphasic or liquid crystal solutions; half-filled circles, data from intrinsic viscosity measurements.



**Figure 5.** Molecular weight dependence of zero-shear viscosity  $\eta_0$  at the concentrations indicated. The figure attached to each straight line indicates the slope.

from Figure 4. The data at  $C = 0.05$  and  $0.10$  g cm<sup>-3</sup> are for rigid-rod samples and show that  $\eta_0$  increases with  $M^7$ - $M^8$  in the rigid-rod regime. Those at  $C = 0.003$  g cm<sup>-1</sup> are only for semiflexible samples, and those at  $C = 0.01$  g cm<sup>-1</sup> are for both rigid and semiflexible samples. In both cases,  $\eta_0$  increases with  $M_v$  approximately as  $M_v^5$ . The more flexible a rod, the smaller the  $M_v$  dependence of  $\eta_0$ .

In any case, rodlike polymers exhibit much stronger molecular weight dependence than  $M^{3.4}$ , which is characteristic of flexible polymers.<sup>25</sup> A similar strong molecular weight dependence has been reported for other rodlike polymer solutions.<sup>3-6</sup> It should be noted in Figure 4 that only a narrow concentration range is available for examining this remarkable molecular weight dependence of  $\eta_0$ . Furthermore, the  $M_v$  dependence becomes less remarkable with increasing molecular weight owing to increasing flexibility. These situations are contrasted with that for flexible polymers where the 3.4 power law holds over wide ranges of concentration and molecular weight.<sup>25</sup>

It can be seen in Figure 4 that the viscosity curves of samples SPG-4, R-4, and H-23 exhibit maxima; the maximum  $\eta_0$  increases with  $M_v$ .<sup>3,8</sup> A similar exponent value of 3.2 was reported by Papkov et al.<sup>4</sup> for *N,N*-dimethylacetamide solutions of poly(*p*-benzamide).

### Discussion

Doi<sup>11</sup> has defined the concentration range referred to as the semidilute concentration regime, in which rodlike polymers entangle with each other but liquid crystal formation is prohibited, by

$$1/L^3 \ll n \ll 1/dL^2 \quad (1)$$

where  $n$  stands for the number of polymer molecules in a unit volume and  $L$  and  $d$  stand for the length and diameter of the rod, respectively. He has derived an equation of zero-shear viscosity  $\eta_0$  in the isotropic region on the basis of the entanglement concept, omitting almost all the numerical coefficients involved. We have followed his derivation, taking these numerical coefficients into consideration, and arrived at the expression

$$\eta_0 \propto \{\pi\eta_s n^3 L^9 / [24 \ln(L/d)]\}(\alpha - ndL^2)^{-2} \quad (2)$$

where  $\eta_s$  is the solvent viscosity and  $\alpha$  a numerical coefficient. Equation 2 has no proportional factor determining the absolute value of  $\eta_0$  on its right-hand side. We let this proportional factor be  $\Phi$  and recast eq 2 in the form

$$\eta_0 / \{[\eta]_R M \eta_s\} = K(CM)^3 / [1 - \beta(CM)^2] \quad (3)$$

$$[\eta]_R = 2\pi N_A L^3 / [45M \ln(L/d)] \quad (4a)$$

$$K = [15N_A^2 / (16M_L^6)](\Phi/\alpha^2), \quad \beta = N_A d / \alpha M_L^2 \quad (4b)$$

where  $N_A$  is the Avogadro number and  $M_L$  the molecular weight of the polymer per unit length. The left-hand side of eq 3 becomes a universal function of the product  $CM$ , provided that  $\alpha$  and  $\Phi$  are constant for a homologous series of polymer samples.

At infinite dilution, the viscosity of a polymer solution is increased only by the existence of individual polymer molecules. At a little higher concentration, hydrodynamic interactions between polymer molecules give rise to an additional viscosity increase. These increases are represented by the  $C^1$  and  $C^2$  terms of the equation defining  $\eta_d$

$$\eta_d = \eta_s [1 + C[\eta] + k'(C[\eta])^2] \quad (5)$$

where  $k'$  is the Huggins constant. At higher concentrations, the entanglement effect plays a dominant role. The Doi theory deals with this effect only. On the assumption that all these effects are additive in  $\eta_0$ , Matheson<sup>24</sup> has proposed

$$\eta_0 = \eta_d + \eta_e \quad (6)$$

where  $\eta_e$  is the term representing the entanglement effect,

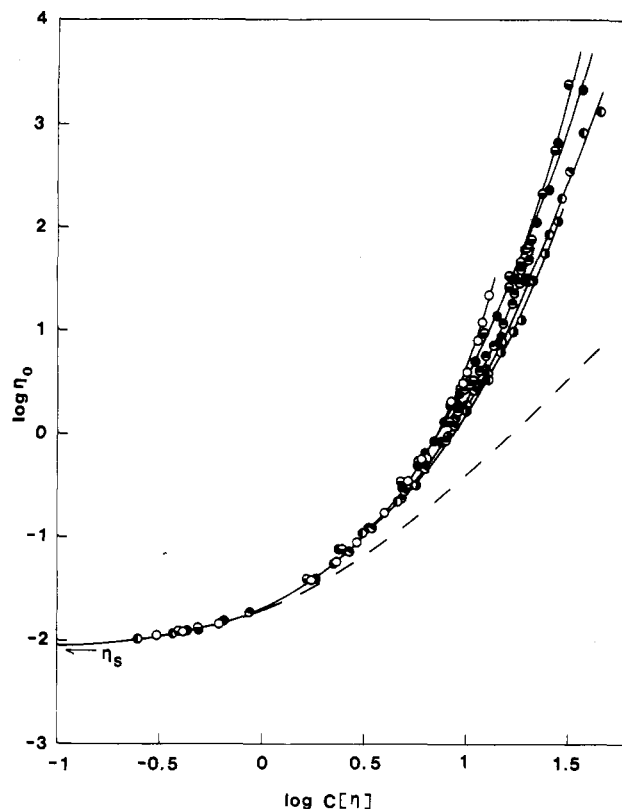


**Figure 6.** Double-logarithmic plots of  $\eta_0$  vs.  $C[\eta]$  for aqueous solutions of seven schizophyllan samples at 30 °C: (○) SPG-4; (●) R-4; (◐) H-23; (◑) E-51; (◒) F-52; (◓) S-53; (◔) N-1. The heavy and the dashed curves represent  $\eta_d$  values calculated by eq 5 with  $k' = 0.40$ .

which should correspond to  $\eta_0$  in the Doi theory. In the following analysis according to the Doi theory, we replace  $\eta_0$  of eq 3 by  $\eta_e$ . Defining  $\eta_{er}$  by

$$\eta_{er} \equiv \eta_e / ([\eta]_R M \eta_s) = K(CM)^3 / [1 - \beta(CM)^2] \quad (7)$$

we obtain

$$\{[\eta]_R M \eta_s (CM)^3 / \eta_{er}\}^{1/2} = \{(CM)^3 / \eta_{er}\}^{1/2} = K^{-1/2} (1 - \beta CM) \quad (8)$$

**Analysis of Schizophyllan Data.** Figure 6 shows plots of  $\eta_0$  for isotropic solutions of all the samples investigated. The heavy curve in the range  $C[\eta] < 1$  and the dashed curve in the range  $C[\eta] > 1$  represent the  $\eta_0$  values calculated by eq 5 with  $k' = 0.4$ . In the former range, the data points for different samples are well superimposed on the heavy curve. However, in the latter range, the data points of each sample deviate largely upward from the dashed curve and follow different thin curves depending on molecular weight. This indicates that the entanglement effect exists only in the range  $C[\eta] > 1$  as far as aqueous schizophyllan is concerned. The difference between the thin and dashed curves at fixed  $C[\eta]$  is a measure of the entanglement effect, which is seen to depend on molecular weight. The following analysis in terms of the Doi theory uses only those  $\eta_{er}$  data satisfying the condition  $C[\eta] > 1$ .

From the above argument, it can be considered that the concentration  $C'$  ( $C[\eta] = 1$ ) corresponds to the lower bound of the semidilute concentration regime; in the previous paper, we regarded the concentration at which  $\eta = 25\eta_s$  as  $C'$ . The upper bound of the regime may be equated to  $C^{**}$ . In Table III, these experimental boundary concentrations are compared with those predicted by eq 1; the predicted values were calculated with  $M_L = 2140 \text{ nm}^{-1}$  and  $d = 1.67 \text{ nm}$ . There are large discrepancies

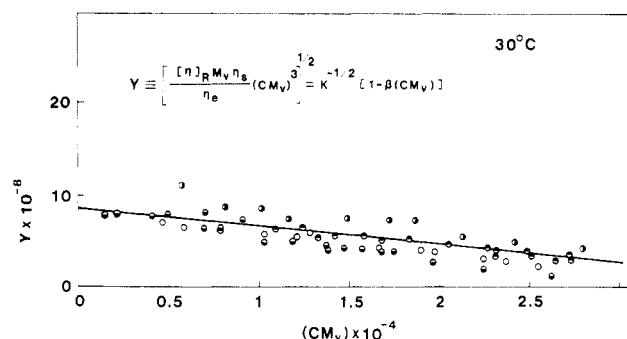


**Figure 7.** Plots of  $Y$  ( $\equiv [([η]_R M_v η_s / η_e (CM_v)^3)^{1/2}]$ ) vs.  $CM_v$  for aqueous solutions of rigid-rod schizophyllan at 30 °C. Symbols have the same meaning as in Figure 6. The straight line shows the least-squares fit to the data points.

**Table III**  
Comparison of Critical Concentrations ( $\text{g cm}^{-3}$ )

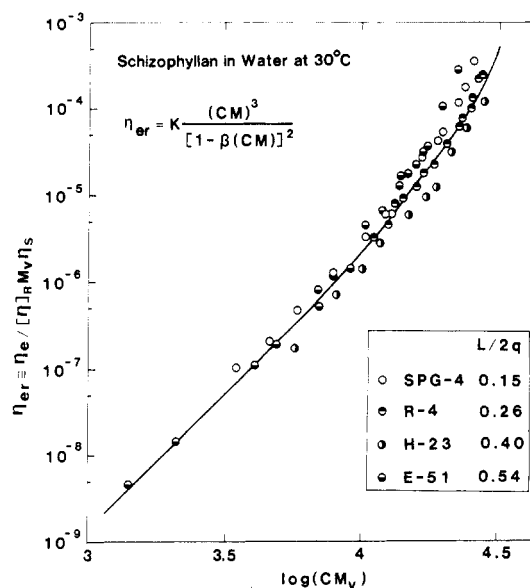
| sample | lower boundary          |                       | upper boundary          |          |
|--------|-------------------------|-----------------------|-------------------------|----------|
|        | eq 1 ( $1/L^3$ )        | $C^*(C[\eta] = 1)$    | eq 1 ( $1/dL^3$ )       | $C^{**}$ |
| SPG-4  | $9.95 \times 10^{-4}$   | $1.56 \times 10^{-2}$ | $3.55 \times 10^{-2}$   | 0.209    |
| R-4    | $3.34 \times 10^{-4}$   | $6.21 \times 10^{-3}$ | $2.07 \times 10^{-2}$   | 0.135    |
| H-23   | $1.41 \times 10^{-4}$   | $2.99 \times 10^{-3}$ | $1.34 \times 10^{-2}$   | 0.112    |
| E-51   | $7.72 \times 10^{-5}$   | $1.85 \times 10^{-3}$ | $9.94 \times 10^{-3}$   |          |
| F-52   | $(1.75 \times 10^{-5})$ | $6.94 \times 10^{-4}$ | $(4.75 \times 10^{-3})$ |          |
| S-35   | $(5.43 \times 10^{-6})$ | $3.41 \times 10^{-4}$ | $(2.63 \times 10^{-3})$ |          |
| N-1    | $(8.77 \times 10^{-7})$ | $1.14 \times 10^{-4}$ | $(1.06 \times 10^{-3})$ |          |

between the experimental and predicted values. This may be due to the lack of proportionality factors in eq 1. (The calculated values differ from those of the previous report<sup>14</sup> because the  $d$  values used are different. However, we see no essential change in the conclusion.) Similar discrepancies are found in other systems.<sup>5</sup>

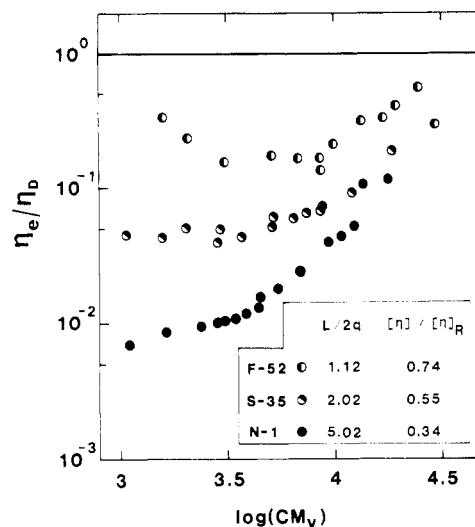
Figure 7 shows the  $\eta_0$  data for rigid-rod samples SPG-4, R-4, H-23, and E-51 plotted according to eq 8;  $\eta_e$  is used instead of  $\eta_0$ . The data points scatter around the straight line that has been determined by the least squares method, with a relative deviation being 24%.  $K$  and  $\beta$  are found to be  $(1.6 \pm 0.2) \times 10^{-18} \text{ cm}^3 \text{ mol g}^{-2}$  and  $(2.5 \pm 0.2) \times 10^{-5} \text{ cm}^3 \text{ mol g}^{-2}$ , respectively.<sup>26</sup> From these  $K$  and  $\beta$  values along with  $M_L = 2140 \text{ nm}^{-1}$  and  $d = 1.67 \text{ nm}$ , we get  $\alpha = 8.8 \pm 0.7$  and  $\Phi = 0.03$ . A value of  $32/\pi$  has been obtained for  $\alpha^*$  theoretically,<sup>24,27</sup> where  $\alpha^*$  is the  $\alpha$  value at the A point. This  $\alpha^*$  value is close to the  $\alpha$  value obtained above. The above  $\Phi$  value is taken to mean that the Doi viscosity equation is accurate to 0.03 relative to unity.

Figure 8 shows  $\eta_{er}$  plotted against  $CM_v$  for samples SPG-4, R-4, H-23, and E-51. The solid curve in the figure represents the theoretical values calculated according to eq 7 with  $K$  and  $\beta$  obtained above. It is seen that the data points for different  $C$  and  $M_v$  are superimposed on the theoretical curve, confirming the validity of eq 7.

Effects of chain flexibility on zero-shear viscosity may be measured by the ratio  $\eta_e/\eta_D$ , where  $\eta_D$  is the viscosity for a rigid-rod molecule calculated by eq 7. Indeed,  $\eta_e/\eta_D$  values for the rigid-rodlike samples were found to be within the range  $0.93 \pm 0.35$ . Figure 9 shows plots of  $\eta_e/\eta_D$  vs.  $CM_v$  for semiflexible samples F-52, S-35, and N-1. The data points of all the samples deviate downward from the horizontal line  $\eta_e/\eta_D = 1$ ; that is, the measured viscosity values are smaller than those predicted for rigid-rodlike polymers. As shown in Table I, sample N-1 is semiflexible and has  $[\eta]$  about one-third of  $[\eta]_R$  for a rod with the same molecular weight. This difference in  $[\eta]$  is 3–30 times amplified in  $\eta_e$ . Similar but less remarkable differences are seen for samples F-52 and S-35. The data points of samples S-35 and N-1 tend to gradually approach the straight line  $\eta_e/\eta_D = 1$  as  $CM_v$  increases. This indicates



**Figure 8.** Plots of  $\eta_{er}$  vs.  $CM_v$  for rigid-rod schizophyllan in water at 30 °C. Symbols have the same meaning as in Figure 6. The solid curve represents theoretical values calculated by eq 7 with  $K = 1.6 \times 10^{-18} \text{ cm}^3 \text{ mol g}^{-2}$  and  $\beta = 2.5 \times 10^{-5} \text{ cm}^3 \text{ mol g}^{-2}$ .



**Figure 9.** Ratios of  $\eta_e$  to  $\eta_D$  plotted against  $CM_v$  for three semiflexible schizophyllan samples F-52 (○), S-35 (●), and N-1 (●).

that the viscosity behavior of a sample having flexibility in dilute solution approaches that of the corresponding rigid-rod sample with increasing concentration.

It is assumed in the Doi theory that although entangled together in semidilute solution, individual rodlike molecules translate along their axes as easily as in dilute solution. This assumption is taken into account by  $\eta_s$  in eq 2, 3, and 7. However, it is well-known that this assumption no longer holds at higher concentrations because of the reduced free volume of the system.<sup>28</sup> It may be possible to take this effect into account by substituting for  $\eta_s$  a concentration-dependent friction coefficient, but at present no information is available about this effect. In the present analysis we have assumed that there is no free volume effect and taken the viscosity of water as  $\eta_s$  for aqueous schizophyllan, whose highest concentration investigated is at most 21%.

**Comparison with Other Polymers.** The parameters  $K$  and  $\beta$  include the physical quantities  $M_L$  and  $d$ , which depend obviously on the polymer and the unknown parameters  $\alpha$  and  $\Phi$ , which may depend on the polymer-solvent system. It is reasonable to take  $\beta CM$  rather than

Table IV  
Parameters Used for Analysis of Viscosity Data<sup>a</sup>

| polymer                    | $M_L$ , nm <sup>-1</sup> | $q$ , nm | $d$ , nm           | $\eta_s$ , <sup>b</sup> P   | $\alpha$          |
|----------------------------|--------------------------|----------|--------------------|---|-------------------|
| schizophyllan <sup>c</sup> | 2140                     | 200      | 1.67 <sup>34</sup> | $7.97_5 \times 10^{-3}$ (water)   | 8.8               |
| PBLG <sup>b,d</sup>        | 1460                     |          | 1.7                | 0.127 ( <i>m</i> -cresol)   | 26.5 <sup>e</sup> |
| PBT <sup>f</sup>           | 220                      |          | 0.9                | 0.104 (MSA)   | 16.2 <sup>e</sup> |
| PBO <sup>f</sup>           | 183                      |          | 0.9                | 0.104 (MSA)   |                   |
| PPTA <sup>f</sup>          | 189                      | 80       | 0.9                | 0.104 (MSA) <sup>f</sup><br>0.23 (H <sub>2</sub> SO <sub>4</sub> ) <sup>g</sup> |                   |

<sup>a</sup> PBT = poly(*p*-phenylene-2,6-benzobisthiazole), PBO = poly(*p*-phenylene-2,6-benzobisoxazole), PPTA = poly(*p*-phenylene-terephthalamide), MSA = methanesulfonic acid. <sup>b</sup>  $[\eta]_R$  for PBLG was estimated from  $[\eta]$  by using the  $[\eta]_R$ - $[\eta]$  relationship given in ref 31. <sup>c</sup> Reference 15. <sup>d</sup> References 30 and 31. <sup>e</sup> Calculated from Figure 10 with  $\Phi$  assumed to be 0.03 (see text). <sup>f</sup> Reference 5. <sup>g</sup> Reference 6.

*CM* as a variable in eq 7 in a comparison among different polymers, because  $\beta$  depends on  $M_L$  and  $d$ . Considering that  $K$  also depends on the system, we rearrange eq 7 to get

$$\eta_{er} d^3 = K' \Phi \alpha (\beta CM)^3 / [1 - (\beta CM)]^2 \quad (9)$$

where  $K' = 15/16N_A$ .

To proceed further, we make the following assumptions on  $\Phi$  and  $\alpha$ :

(1)  $\Phi$  is regarded as a universal constant independent of the system because  $\eta_e$  may originate in the topological restriction against molecular motion due to the rodlike shape of a molecule.

(2)  $\alpha$  is approximately constant because it is a geometrical factor that provides the relation among  $L$ ,  $d$ ,  $n$  and the effective region in a tube in which a rod can move freely. Under these assumptions,  $K' \Phi \alpha$  in eq 9 is a constant.

In a comparison of  $\eta_e$  among different systems, we choose a reference system and represent the quantities associated with it by a subscript 0. Equation 9 suggests that a plot of  $\eta_{er}$  vs.  $CM$  for a given system should be shifted by  $(d/d_0)^3$  along the ordinate and by  $(\beta/\beta_0)$  along the abscissa compared with that of the reference system. The resulting plots for different rodlike polymers should form a single composite curve. In the previous paper,<sup>14</sup>  $\eta_{er}$  was reduced by  $(\beta/\beta_0)^3$ . However, the previous argument based on this reduction is not correct, since  $\eta_{er}$  contains  $M_L$ , which depends on the polymer species. A reduced plot suggested by Berry et al.<sup>29</sup> may not be correct for a similar reason. The previous Figure 8 and the associated arguments should be revised as Figure 10 and the discussion to follow. We chose aqueous schizophyllan in the rigid-rod regime as the reference system in the following analysis.

Figure 10 shows the plot of  $\eta_{er}(d/d_0)^3$  vs.  $(\beta/\beta_0)(CM)$  for the data of polymers other than schizophyllan. PBLG is an  $\alpha$ -helix-forming polypeptide and rigid at molecular weights lower than ca. 200 000.<sup>30</sup> PBT and PBO are rigid main-chain heterocyclic polymers.<sup>5</sup> PPTA<sup>5,6</sup> is a rigid polymer well-known as Kevlar.  $M_v$ (PBLG) or  $M_w$ (PBLG, other polymers) are used for  $M$ . For PBLG, values of  $[\eta]_R$  were estimated on the basis of an analysis by Itou et al.<sup>31</sup> and the values  $\eta_e$  were calculated with  $k' = 0.40$ . For the other polymers,  $\eta_0$  and  $[\eta]$  were used instead of  $\eta_e$  and  $[\eta]_R$ , respectively, because no data were available to calculate  $\eta_e$  and  $[\eta]_R$ . The parameters used for the calculation are listed in Table IV. The heavy line labeled "Schizophyllan" is the theoretical curve determined for schizophyllan in Figure 7.

It is seen in Figure 10 that the data points for rigid-rod polymers PBT and PBLG A-15, H-22, and Y-20 appear

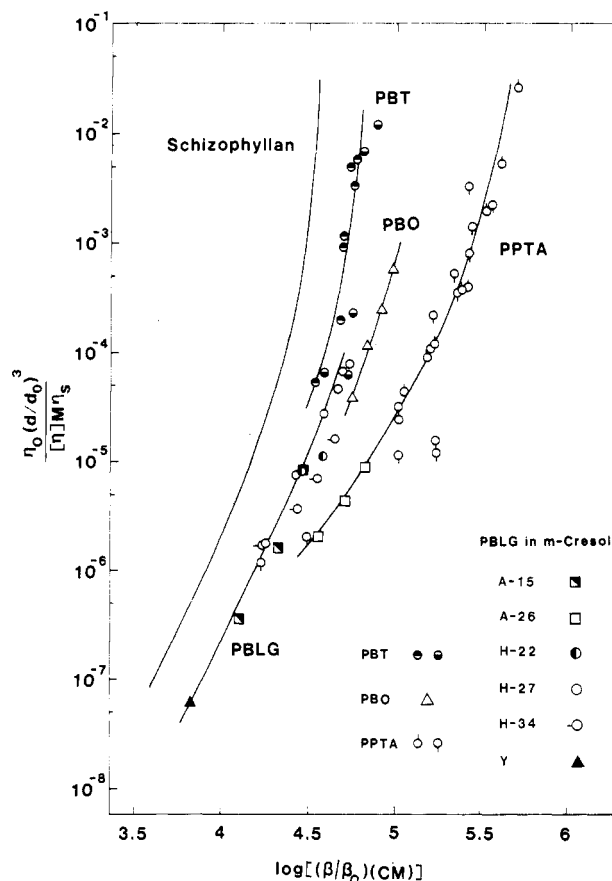


Figure 10. Reduced plots of  $[\eta_0(d/d_0)^3]$  vs.  $(\beta/\beta_0)(CM)$  for various polymer-solvent systems: poly(*p*-phenylene-2,6-benzobisthiazole) (PBT) in methanesulfonic acid (MSA) ( $\bullet$ ), Chu et al.;<sup>5</sup> PBT in MSA + 3% chlorosulfonic acid ( $\odot$ ), Chu et al.;<sup>5</sup> poly(*p*-phenylene-2,6-benzobisoxazole) (PBO) in MSA ( $\Delta$ ), Chu et al.;<sup>5</sup> poly(*p*-phenyleneterephthalamide) (PPTA) in MSA ( $\diamond$ ), Chu et al.;<sup>5</sup> PPTA in 100% sulfuric acid ( $\circ$ ), Baird and Ballman;<sup>6</sup> poly( $\gamma$ -benzyl L-glutamate) (PBLG) in *m*-cresol ( $\blacksquare$ ,  $\square$ ), Asada et al.;<sup>7</sup> PBLG in *m*-cresol ( $\bullet$ ,  $\circ$ ,  $\odot$ ), Hermans;<sup>3</sup> PBLG in *m*-cresol ( $\blacktriangle$ ), Yang.<sup>32</sup> The curve labeled "Schizophyllan" shows the theoretical values for aqueous schizophyllan taken as the reference. The sample code A-*n* and H-*n* for PBLG indicates that the molecular weight of the sample is about  $n \times 10^4$ .

plotted definitely below the theoretical curve and also at abscissa values larger than 4.65, where the theoretical value diverges. This indicates that  $\alpha$  or  $\Phi$  or both of them for these systems are different from those of aqueous schizophyllan. The data points for PBT and PBLG can be superimposed on the theoretical curve if  $\alpha$  is taken to be 16.2 for PBT and 26.5 for PBLG, with  $\Phi$  being held constant. The heavy curve for each polymer is the theoretical curve corresponding to each  $\alpha$  value. The accuracies of these values are only moderate. The superposition can be made by varying  $\alpha$  and  $\Phi$  at the same time but not by varying  $\Phi$  alone. Thus assumptions 1 and 2 may not be satisfied rigorously with experimental data. The slopes of the curves for PBO and PPTA are smaller than that of PBT. It may be because PBO and PPTA are not as rigid as PBT.<sup>5,33</sup> However, this reasoning must be taken with some reservation because association may be another reason for this disparity.<sup>5</sup>

### Concluding Remarks

According to eq 7, the slope of a double-logarithmic plot of  $\eta_{er}$  vs.  $CM$  should be 3 at small  $CM$  and increase with increasing  $CM$ . To test eq 7 and get a reasonable estimate of  $\alpha$ ,  $\eta_{er}$  should be obtained in such a wide  $CM$  range that this plot shows a significant curvature for a polymer in the



rigid-rod regime. Neither of the data by the previous authors satisfy these two requirements. This is why an independent estimate of  $\alpha$  and  $\Phi$  has not been attempted for their data. Finally, we find no theoretical justification for the experimental  $\Phi$  removed from unity and diversity of  $\alpha$  among different polymers. The need for further theoretical study is indicated.

**Acknowledgment.** We acknowledge gratefully the partial support of Idemitsu Kosan Co., Ltd. through a research grant.

**Registry No.** Schizophyllan, 9050-67-3.

## References and Notes

- (1) Robinson, C. *Trans. Faraday Soc.* **1956**, *52*, 571.
- (2) Robinson, C.; Ward, J. C.; Beevers, R. B. *Discuss. Faraday Soc.* **1958**, *25*, 29.
- (3) Hermans, J., Jr. *J. Colloid Sci.* **1962**, *17*, 638.
- (4) Papkov, S. P.; Kulichikhin, V. G.; Kalmykova, V. D.; Malkin, A. Ya. *J. Polym. Sci., Polym. Phys. Ed.* **1974**, *12*, 1753.
- (5) Chu, S. G.; Venkatraman, S.; Berry, G. C.; Einaga, Y. *Macromolecules* **1981**, *14*, 939.
- (6) Baird, D. G.; Ballman, R. L. *J. Rheol. (N.Y.)* **1979**, *23*, 505.
- (7) Asada, T.; Yanase, H.; Onogi, S. *Polym. Prepr. Jpn.* **1982**, *31*, 1893.
- (8) Morgan, P. W. *Macromolecules* **1977**, *10*, 1381.
- (9) Kwolek, S. L.; Morgan, P. W.; Schaefgen, J. R.; Gulrich, L. W. *Macromolecules* **1977**, *10*, 1390.
- (10) Aharoni, S. M. *J. Polym. Sci., Polym. Phys. Ed.* **1980**, *18*, 1439.
- (11) Doi, M. *J. Phys. (Les Ulis, Fr.)* **1975**, *36*, 607.
- (12) Doi, M. *J. Polym. Sci., Polym. Phys. Ed.* **1981**, *19*, 229.
- (13) Berry, G. C. *J. Polym. Sci., Polym. Symp.* **1980**, No. 34, 43.
- (14) Enomoto, H.; Einaga, Y.; Teramoto, A. *Macromolecules* **1984**, *17*, 1573.
- (15) Yanaki, T.; Norisuye, T.; Fujita, H. *Macromolecules* **1980**, *13*, 1462.
- (16) Norisuye, T.; Yanaki, T.; Fujita, H. *J. Polym. Sci. Polym. Phys. Ed.* **1980**, *18*, 547.
- (17) Itou, T.; Van, K.; Teramoto, A. *J. Appl. Polym. Sci., Appl. Polym. Symp.* **1985**, *41*, 35.
- (18) Van, K.; Norisuye, T.; Teramoto, A. *Mol. Cryst. Liq. Cryst.* **1981**, *78*, 123.
- (19) Van, K.; Teramoto, A. *Polym. J. (Tokyo)* **1982**, *14*, 999.
- (20) Einaga, Y.; Miyaki, Y.; Fujita, H. *J. Polym. Sci., Polym. Phys. Ed.* **1979**, *17*, 2103.
- (21) Einaga, Y.; Miyaki, Y.; Fujita, H. *J. Soc. Rheol., Jpn.* **1977**, *5*, 188.
- (22) Kashiwagi, Y.; Norisuye, T.; Fujita, H. *Macromolecules* **1981**, *14*, 1220.
- (23) These  $\eta_0$  values may be regarded as those in the plateau regions, although no plateau region is seen in the actual data because of the limited range of torque available.
- (24) Matheson, R. R., Jr. *Macromolecules* **1980**, *13*, 643.
- (25) Ferry, J. D. "Viscoelastic Properties of Polymers", 3rd ed.; Wiley: New York, 1980; Chapter 10.
- (26) These  $K$  and  $\beta$  values have been determined by the least-squares method so as to minimize the mean square of relative difference from the theoretical values. They are different from those reported in our previous paper.<sup>14</sup> This is because the analysis was made on the whole data, including those for samples R-4 and H-23 together with a  $d$  value different from the previous one.
- (27) Valiev, K. A.; Ivanov, E. N., *Sov. Phys.-Usp. (Engl. Transl.)* **1973**, *16*, 1.
- (28) Ferry, J. D., ref 25, Chapter 17.
- (29) Berry, G. C.; Venkatraman, S.; Einaga, Y. *Proc. IUPAC, I. U.P.A.C. Macromol. Symp.*, **28th** **1982**, 790.
- (30) Teramoto, A.; Fujita, H. *Adv. Polym. Sci.* **1975**, *18*, 65.
- (31) Itou, S.; Nishioka, N.; Norisuye, T.; Teramoto, A. *Macromolecules* **1981**, *14*, 904.
- (32) Yang, J. T. *J. Am. Chem. Soc.* **1958**, *80*, 1783.
- (33) Metzger, P. Ph.D. Thesis, Carnegie-Mellon University, Pittsburgh, PA, 1979.
- (34) In the present analysis,  $d$  is taken to be 1.67 nm, the value calculated from the partial specific volume of schizophyllan in water,<sup>16</sup> because  $\alpha$  and  $d$  may be regarded as the thermodynamic parameters determining the spatial distribution of rod-like molecules in solution. Use of the hydrodynamic diameter 2.6 nm gives  $\alpha = 12.8 \pm 1$  and  $\Phi = 0.05$ .

## Motional Correlation Times of Nitroxide Spin Labels and Spin Probes in an Amine-Cured Epoxy Resin: Solvent Dependence

I. M. Brown\* and T. C. Sandreczki

McDonnell Douglas Research Laboratories, St. Louis, Missouri 63166.

Received December 17, 1984

**ABSTRACT:** Nitroxide spin labels and spin probes have been used to investigate the microstructure in the polymer network of an amine-cured epoxy resin. The behavior of the electron paramagnetic resonance (EPR) line shapes of the nitroxides was studied as a function of solvent plasticizer content. At low solvent contents ( $\leq 5$  wt %) the line shape was a slow-phase spectrum that differed little from that in the dry sample, whereas at high solvent contents ( $\geq 30$  wt %) the line shape was a fast-phase spectrum similar to the typical motionally narrowed spectrum. Over a range of intermediate solvent contents, the line shape was a superposition of a slow-phase and a fast-phase spectrum where the motional correlation times characterizing these spectra differed by more than 1.5 orders of magnitude. The slow phase is identified with nitroxides located in regions of high cross-link density, whereas the fast phase is attributed to nitroxides in regions of lower cross-link density that have been selectively plasticized by the solvent. The mobile fraction of the spin labels, evaluated from the areas under the fast- and slow-phase absorption spectrum, is a crude measure of the distribution of cross-link density in the epoxy network.

## Introduction

Epoxy resin polymers are used as matrix materials for composite structural components in the aerospace industry. At present there is considerable evidence to suggest that the polymer network in cured epoxy resins contains regions of nonuniform cross-link density.<sup>1-7</sup> These network inhomogeneities consist of regions of high cross-link density, variously referred to as globules,<sup>2</sup> nodules,<sup>3</sup> or domains,<sup>7</sup> embedded in and bound to regions of lower cross-link density. It is important to characterize these

network inhomogeneities because of the consequences of network morphology on mechanical properties such as yield strength and toughness.

In this study we have used electron paramagnetic resonance (EPR) spectroscopy to obtain information about this network microstructure. Since the epoxy resins are diamagnetic, nitroxide free radicals<sup>8</sup> were used as paramagnetic probes of their dynamic local environments in the polymers. The nitroxide was employed either as a spin label, where it was covalently bound at a known site in the